Nanoscale Research Letters
a SpringerOpen Journal

NANO EXPRESS Open Access

Improvement of carrier diffusion length in silicon nanowire arrays using atomic layer deposition

Shinya Kato[1*], Yasuyoshi Kurokawa[1,2], Shinsuke Miyajima[1], Yuya Watanabe[1], Akira Yamada[1,3], Yoshimi Ohta[4], Yusuke Niwa[4] and Masaki Hirota[4]

Abstract

To achieve a high-efficiency silicon nanowire (SiNW) solar cell, surface passivation technique is very important because a SiNW array has a large surface area. We successfully prepared by atomic layer deposition (ALD) high-quality aluminum oxide (Al_2O_3) film for passivation on the whole surface of the SiNW arrays. The minority carrier lifetime of the Al_2O_3-depositedSiNW arrays with bulk silicon substrate was improved to 27 μs at the optimum annealing condition. To remove the effect of bulk silicon, the effective diffusion length of minority carriers in the SiNW array was estimated by simple equations and a device simulator. As a result, it was revealed that the effective diffusion length in the SiNW arrays increased from 3.25 to 13.5 μm by depositing Al_2O_3 and post-annealing at 400°C. This improvement of the diffusion length is very important for application to solar cells, and Al_2O_3 deposited by ALD is a promising passivation material for a structure with high aspect ratio such as SiNW arrays.

Keywords: Silicon nanowire; Passivation; Atomic layer deposition; Lifetime; Simulation; Diffusion length

Background

Silicon nanowire (SiNW) enables us to tune the bandgap by the quantum size effect [1] and effective photo-absorption owing to strong optical confinement effect [2-4]. It is possible to apply SiNW to all-silicon tandem solar cells to utilize the broadband solar spectrum at low cost. When a crystalline silicon (1.12 eV) bottom cell is combined with a top cell with SiNW (1.74 eV) [1], all-silicon tandem solar cells have the possibility to overcome the Shockley-Queisser limit [5]. Moreover, it is expected that SiNW solar cells have higher photocurrent than crystalline silicon solar cell with the same thickness as the SiNW length owing to the higher absorption coefficient derived from optical confinement [6]. SiNW has been prepared by several top-down or bottom-up methods [7-13]. Over the past few years, many researchers have applied SiNWs to solar cells [14-19] for the purpose of optical confinement. We have proposed a SiNW solar cell with a heterojunction structure as shown in Figure 1 [1]. When SiNW arrays are applied to such a solar cell, it is significantly important to reduce the surface recombination velocity of the SiNW surface by using passivation films since the large surface area of SiNWs enhances minority carrier recombination at the surface. However, there are a few reports about the passivation of silicon nanowires to reduce surface recombination velocities, which determine the performance of solar cells. Dan et al. have reported the passivation effect of a thin layer of amorphous silicon on a single-crystalline silicon nanowire prepared by the Au-catalyzed vapor–liquid-solid (VLS) process [20]. They showed that the surface recombination velocity was reduced by amorphous silicon by nearly 2 orders of magnitude. Demichel et al. have demonstrated that surface recombination velocities as low as 20 cm/s were measured for SiNWs prepared by the same process and efficiently passivated by a thermal oxidation [21]. Although these results are based on SiNWs prepared by the VLS process, considering application to solar cells, metal-assisted chemical etching is more promising [11,18,22-25] since vertical SiNW arrays can be prepared in a large area under no vacuum. However, there is no report on the deposition of passivation films and their passivation effect on SiNW arrays prepared by the MAE process. Moreover, no result has ever been reported on minority carrier lifetime in vertical SiNW arrays to

* Correspondence: kato.s.am@m.titech.ac.jp
[1]Department of Physical Electronics, Tokyo Institute of Technology, Meguro-ku, Tokyo 152-8552, Japan
Full list of author information is available at the end of the article

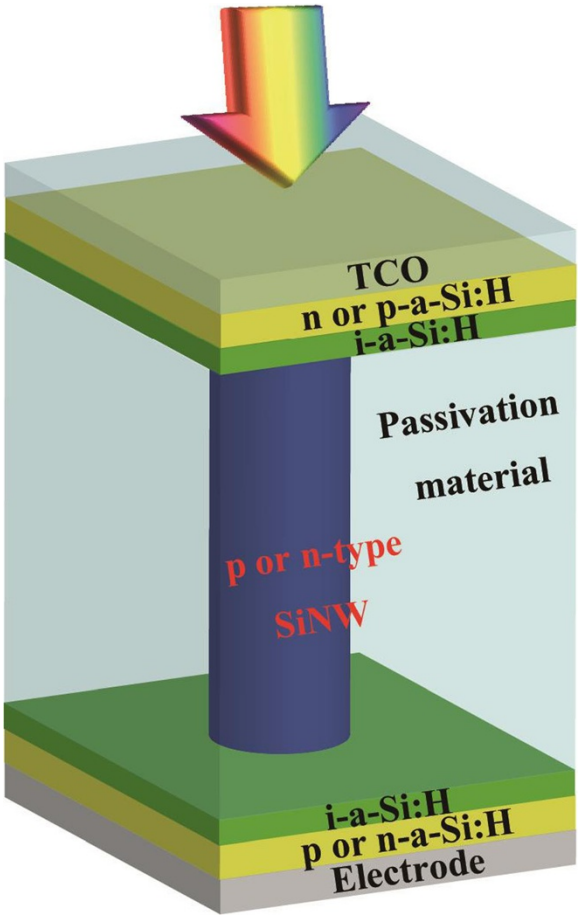

Figure 1 The SiNW solar cell structure that we have proposed.

estimate passivation effect. Minority carrier lifetime is the dominant factor affecting the characteristics of solar cells. Therefore, it is important to measure minority carrier lifetime to analyze the characteristics of solar cells. In our previous work, we successfully fabricated 30-nm-diameter SiNW arrays by metal-assisted chemical etching using silica nanoparticles (MACES) [23]. It is well known that aluminum oxide (Al_2O_3) deposited by atomic layer deposition (ALD) [26-29] and hydrogenated amorphous silicon (a-Si:H) deposited by plasma-enhanced chemical vapor deposition (PECVD) [29,30] show an excellent surface passivation effect on crystalline silicon. In this study, we investigated the deposition of a-Si:H by PECVD and $Al_2O_3$by ALD around SiNW arrays and measured the minority carrier lifetime in SiNW arrays by the microwave photo-conductivity decay (μ-PCD) method. However, the measured minority carrier lifetime was influenced by the supporting crystalline silicon substrate underneath the SiNWs. We carried out numerical simulations using PC1D (University of NSW) [31-33] simulation software to extract the minority carrier lifetime in the SiNW array layer, assuming that the SiNW layer is a homogeneous single-phase material with a minority carrier lifetime. Based on the simulation results, we proposed a simple equation to extract the minority carrier lifetime in the SiNW layer from measured minority lifetime.

Methods

Si wafers (p-type, (100), 2 to 10 Ω cm) were used for the fabrication of SiNW arrays. The surfaces of the Si wafers were hydrophilic by modifying with an amino group. The hydrophilic Si wafers were immersed in a solution in which 30-nmsilica nanoparticles modified with a carboxyl group were dispersed at 2°C for 1 h. This process formed a dispersed silica nanoparticle layer on the Si wafer. Subsequently, a 20-nm-thick silver film was deposited on the wafers with silica nanoparticles using a DC sputtering system. After removing the silica nanoparticles by ultrasonication in deionized water, Si wafers with a nano-patterned silver film were obtained. The wafer was chemically etched using 4.8 M HF and 0.15M H_2O_2 at room temperature to form SiNW arrays. The remaining silver film on the bottom of the SiNW arrays was removed by HNO_3 wet etching. Finally, the oxide layer existing on the surface of the SiNW array was removed with a HF solution. Details of the SiNW array fabrication process are shown elsewhere [23]. After the fabrication of SiNW arrays, intrinsic amorphous silicon was deposited by PECVD under the same condition as the heterojunction crystalline silicon solar cell in which the fabrication temperature is 210°C and the operating pressure is 0.3 Torr. After the deposition, the SiNW array was annealed in a forming gas at 200°C, which is the best annealing temperature for the surface passivation of our a-Si:H. On the other hand, Al_2O_3 was also deposited using $Al(CH_3)_3$ and H_2O alternately at 200°C by an ALD system. After the deposition, the SiNW arrays were annealed in a forming gas at 400°C. These nanostructures of the prepared SiNW arrays were characterized by field emission scanning electron microscopy (SEM) and energy-dispersive X-ray spectroscopy (EDS) with JEOL JSM-7001F (JEOL, Tokyo, Japan). The structure of the interface between SiNW and Al_2O_3 was observed by transmission electron microscopy (TEM) with HITACHI H-9000NAR (HITACHI, Tokyo, Japan) and high-angle annular dark field scanning transmission electron microscopy (HAADF-STEM) with HITACHI HD-2700. Minority carrier lifetime was measured by the μ-PCD method with KOBELCO LTE-1510EP (KOBELCO, Tokyo Japan).

To investigate the carrier lifetime in a SiNW region (τ_{SiNW}), one-dimensional numerical simulations were carried out using PC1D. The electrical transport was calculated by solving Poisson equations and carrier continuity equations. In the simulations, we employed a

simple structure in which a homogeneous single-phase material with a small carrier lifetime is stacked on a crystalline silicon substrate with a large carrier lifetime as shown in Figure 2. The homogeneous single-phase material is equivalent to the SiNW region. We calculated the effective minority carrier lifetime in the structure (τ_{whole}) as a function of the minority carrier lifetime in the equivalent SiNW region (τ_{SiNW}) to investigate the relationship between τ_{whole} and τ_{SiNW}. τ_{whole} corresponds to the measured effective lifetime (τ_{eff}). Electrical parameters used in our simulations are summarized in Table 1. The absorption coefficient of a SiNW was used with the same value as crystalline silicon because it has not been confirmed by an experiment yet. The wavelength of an incident light was 904 nm, which is the same as the wavelength of the laser used in μ-PCD measurement. Moreover, Shockley-Read-Hall recombination, Auger recombination, and band-to-band recombination were taken into account, and the surface recombination was neglected for simplification.

Results and discussion

The decay curve of SiNW arrays fabricated by MACES was successfully obtained from μ-PCD measurement, as shown in Figure 3a. From Figure 3b, we confirmed that the decay curve consisted of two components, which were fast-decay and slow-decay components. At present, the origin of the second slow-decay component is not clear. A possible explanation is that the slow decay originates from minority carrier trapping effect at the defect states on the surface of the SiNW arrays. As a result of fitting to exponential attenuation function, the τ_{eff} of the SiNW arrays on the Si wafers is found to be 1.6 μs. This low τ_{eff} reflects the large surface recombination velocity at the surface of the SiNW arrays because we used high-quality crystalline silicon wafer as starting materials. To improve τ_{eff}, passivation films were deposited on the SiNW arrays. In the case of the a-Si:H passivation film, τ_{eff} was not improved since only a small part of the SiNW arrays was covered with the a-Si:H film. The a-Si:H thin film was deposited only on top of the SiNW array owing to the high density of SiNWs as shown in Figure 4. This reason can be explained according to the studies of Matsuda et al., in which they reported about the deposition of a-Si:Hon trench structure by PECVD [34,35]. The concentration of precursors related with a silane gas decreased as their position on the SiNW moved farther from the plasma region, suggesting that the precursors could not reach the bottom of the SiNWs. That is why the a-Si:H thin film was deposited only on top of the SiNW array. In fact, the interspace between our fabricated SiNWs could not be embedded owing to the very narrow gap at around 20 nm. On the other hand, in the case of SiNW arrays covered with the as-deposited Al_2O_3 film, the τ_{eff} increased to 5 μs. That is because the surface of the SiNW arrays was successfully covered with Al_2O_3. In Figure 5a, the cross-sectional SEM images of the SiNW array before and after the deposition of an Al_2O_3 passivation film are shown. After the deposition of Al_2O_3, the dark contrast owing to the gap between SiNWs disappeared, suggesting that the Al_2O_3 film macroscopically covered SiNWs. Figure 5b,c shows the EDS mappings of aluminum and silicon, respectively. White and black signals show a maximum and minimum value, respectively. Note that the signal of aluminum was detected on the bottom of SiNWs after Al_2O_3 deposition, although the signal was not detected before the deposition. However, the Al intensity around the bottom was weaker than the one at the top. From a SEM image, the shape of SiNWs around the top is needle-like and the gap between SiNWs is about several hundred nanometers, although the gap around the bottom is about several ten nanometers (not shown). Therefore, the intensity of Al is higher around the top. These results also suggest that the Al_2O_3 film macroscopically covered SiNWs from the top to the bottom.

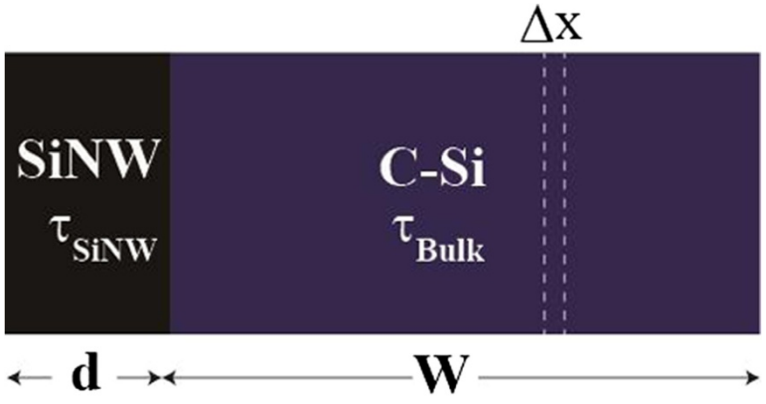

Figure 2 The schematic diagram of the calculation model.

Table 1 Physical parameters for lifetime estimation based on our simple calculation model and PC1D

Symbol	Parameter	Silicon nanowire	Bulk silicon
d, *W*	Length, thickness	10 μm	190 μm
E	Dielectric constant	11.4	11.4
Eg	Energy gap (eV)	1.12	1.12
χ	Electron affinity (eV)	4.05	4.05
Dt	Trap level	0	0
τ_{e0}, τ_{h0}	Carrier lifetime	0.05 to 1.5 μs	1 ms
μ_e	Electron mobility ($cm^2/(Vs)$)	1,104	1,104
μ_h	Hole mobility ($cm^2/(Vs)$)	424.6	424.6
N_A	Accepter concentration (cm^{-3})	1×10^{16}	1×10^{16}

To investigate the microscopic structure of the interface between a SiNW and Al_2O_3, TEM and HAADF-STEM observations were carried out. Figure 6a,b shows a schematic diagram on how to fabricate the sample for HAADF observation and a HAADF image of the SiNW cut into a round slice at the bottom of the SiNW, respectively. The contrast of a HAADF image is proportional to the square of the atomic number and becomes brighter with increasing atomic number. The contrast between the SiNW and Al_2O_3 is very clear in the figure. It should be noted that there is no gap at the interface. In Figure 6c, the uniform thickness of Al_2O_3 can be seen and is about 30 nm, which is enough for the passivation of crystalline silicon solar cells [29]. The uniform deposition on the SiNW arrays is due to the excellent surface coverage of ALD techniques. From these results, the Al_2O_3 film deposited by the ALD method was able to cover the SiNW arrays up to the bottom. Since the fine interface between a SiNW and Al_2O_3 was formed and dangling bonds on the surface were modified by oxygen, the minority carrier lifetime in the SiNW arrays was improved.

For further improvement of carrier lifetime, annealing of the SiNW arrays embedded in Al_2O_3 was carried out. It was reported that negative fixed charge density at the interface of Al_2O_3/p-type c-Si increased from 1.3×10^{11} to 2.45×10^{12} cm^{-2} by annealing at 400°C [36]. This increase of fixed charge density increases electric field at the Al_2O_3/SiNW interface. The electric field effectively repels minority carrier from the interface, resulting in the increase of minority carrier lifetime in the SiNW arrays. However, if a SiNW has perfect cylindrical symmetry, and Al_2O_3 with negative fixed charge is deposited on the surface uniformly, the electric field in the SiNW will be cancelled due to the symmetry of the electric field. Since in this case the effect of field effect passivation cannot be obtained, the effective lifetime will not be improved by annealing. To confirm the hypothesis, we tried to anneal the SiNW arrays with Al_2O_3 at 400°C. As a result, our SiNW samples also showed improvement of effective minority carrier lifetime, as well as a flat c-Si substrate passivated by Al_2O_3 layers, after annealing at 400°C. The τ_{eff} was found to be 27 μs. From this result, we conclude that since the prepared SiNWs

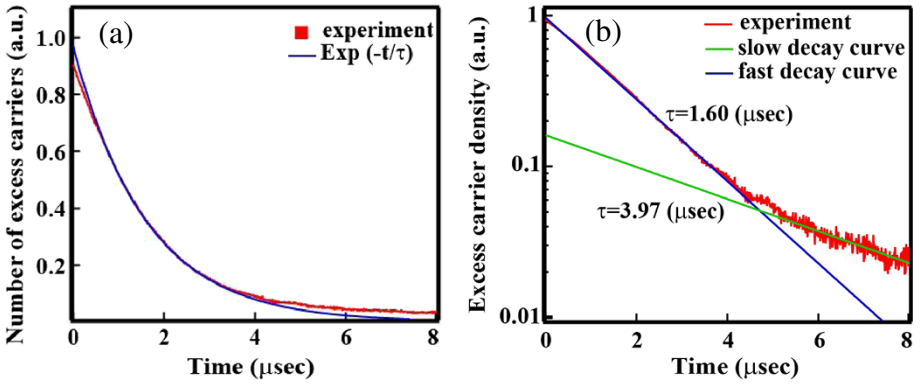

Figure 3 Transient response of excess carrier density in a SiNW array on bulk silicon. (a) Linear scale. **(b)** Logarithmic scale.

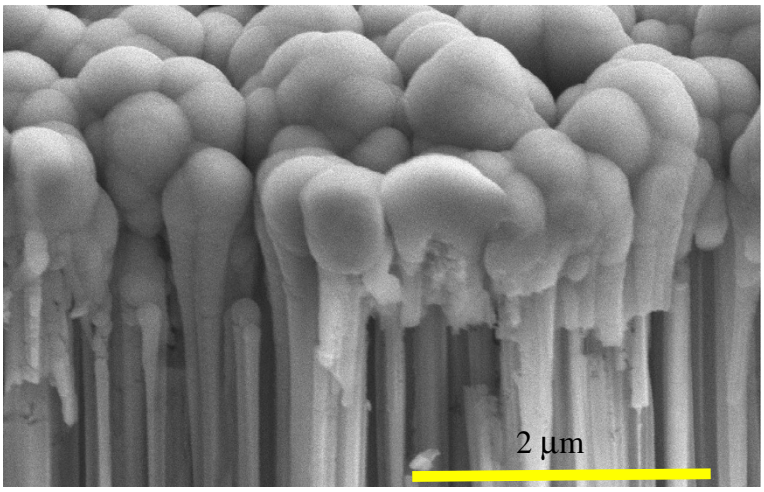

Figure 4 Cross-sectional SEM image of an a-Si:H thin film deposited on a SiNW array.

do not have a perfect cylindrical symmetry, the effect of field effect passivation can be successfully obtained. Since negative charge density in the Al_2O_3 was increased by annealing at 400°C, the effective lifetime was also improved.

Although τ_{eff} of the SiNW arrays on the Si wafers were successfully obtained, we cannot consider these lifetimes as the lifetime of the SiNW region (τ_{SiNW}) due to the influence of the Si wafers. Therefore, we tried to extract τ_{SiNW} from τ_{eff} using PC1D simulation. PC1D simulations revealed that τ_{eff} was significantly influenced by the Si wafers. The calculated τ_{whole} which is equivalent to the measured τ_{eff} is 20 times higher than τ_{SiNW}, as shown in Figure 7. These simulations clearly indicate that the measured τ_{eff} is completely different from τ_{SiNW}.

We proposed a simple equation to extract τ_{SiNW} from τ_{eff} without numerical simulations. In the simulations of PC1D, minority carrier continuity equations were used. In general, the terms of drift, diffusion, recombination, and photogeneration have to be considered in the continuity equations. However, the terms of electric field and photogeneration can be eliminated. In μ-PCD measurement, a decay of excess carrier density is measured after stopping a laser irradiation. Therefore, photogeneration can be neglected. Although negative charge in Al_2O_3 can form electric field on the surface of SiNWs, the influence of the electric charge on excess carriers is limited only on the surface. Therefore, in this calculation, electric field was neglected for simplification. It was assumed that carriers were generated uniformly in the whole region because the carrier density remained alternated by time variation from the resulting PC1D. Therefore, the term diffusion current can be also neglected, and only the recombination current in continuity equations can be considered. The recombination current in infinitesimal difference $\Delta x(J)$ is given by

$$J = q\frac{dn}{dt}\Delta x = -q\frac{n}{\tau}\Delta x \tag{1}$$

where q is the elementary charge, n is the density of electron, and τ is the lifetime. If the lifetimes of SiNW and bulk silicon are taken in account, the recombination current in the whole region is represented by

$$J_{total} = J_{SiNW} + J_{Bulk} = -en\left(\frac{d}{\tau_{SiNW}} + \frac{W}{\tau_{Bulk}}\right) \tag{2}$$

where d is length the of a SiNW, W is the thickness of bulk silicon, τ_{SiNW} is the lifetime of a SiNW, and τ_{Bulk} is the lifetime of bulk silicon. On the other hand, when the effective lifetime is considered as the whole region lifetime (τ_{whole}), the recombination current in the whole region is given by

$$J_{total} = -en\left(\frac{d+W}{\tau_{whloe}}\right) \tag{3}$$

From Equations 2 and 3,

$$-en\left(\frac{d}{\tau_{SiNW}} + \frac{W}{\tau_{Bulk}}\right) = -en\left(\frac{d+W}{\tau_{whole}}\right) \tag{4}$$

The τ_{SiNW} was calculated by

$$\tau_{SiNW} = \frac{d}{\left(\frac{d+W}{\tau_{whole}} - \frac{W}{\tau_{Bulk}}\right)} \tag{5}$$

Figure 7 shows the lifetime of the SiNW arrays which was calculated from the Equation 5 as a function of the lifetime in the whole region when d, W, and τ_{Bulk} are 10 μm, 190 μm, and 1 ms, respectively. For confirmation of

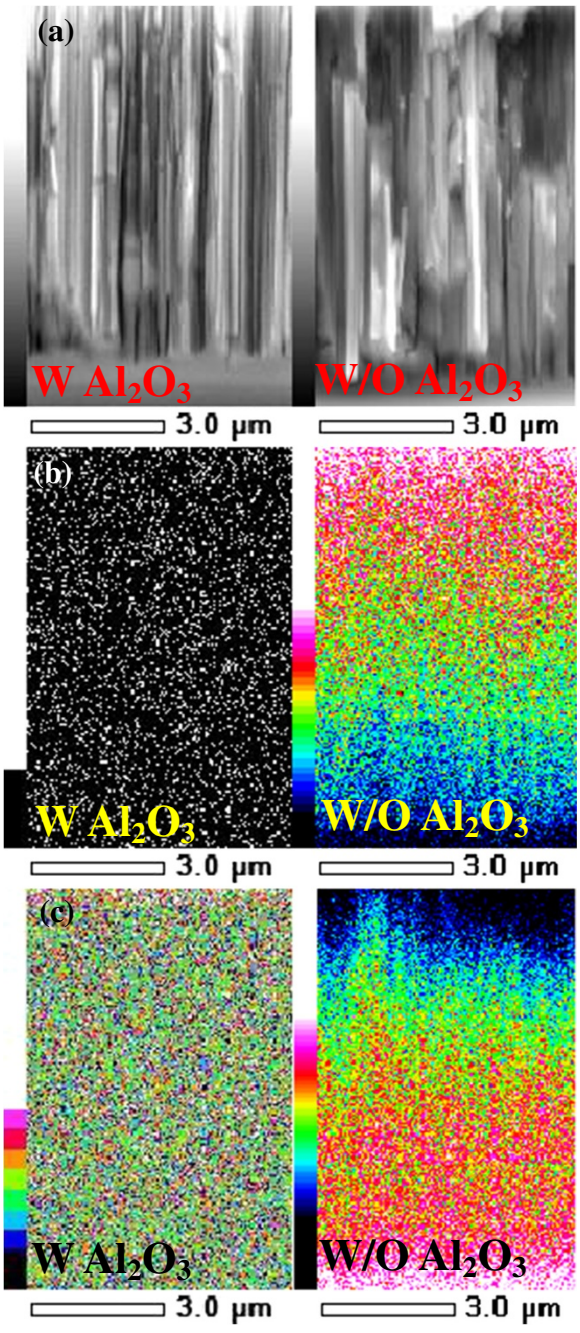

Figure 5 SEM image and EDS mapping of SiNW without and with Al_2O_3. **(a)** Cross-sectional SEM image of SiNWs without and with Al_2O_3. EDS mappings of **(b)** Al and **(c)** Si corresponding to the SiNWs shown in **(a)**, respectively.

validation of this calculation, the τ_{SiNW} obtained by Equation 5 was compared to the simulation results of PC1D in Figure 7. We confirmed that the τ_{SiNW} using PC1D is in good agreement with the calculation based on Equation 5, and it was revealed that the τ_{SiNW} can be extracted by a simple equation such as Equation 5.

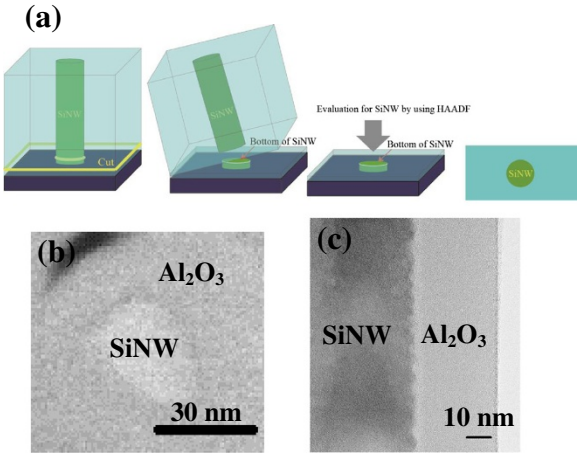

Figure 6 HAADF-STEM and TEM images of the SiNW with Al_2O_3. **(a)**The procedure on how to measure the HAADF-STEM image. **(b)** Cross-sectional HAADF-STEM image of a SiNW cut into a round slice at the bottom of the SiNW array. **(c)** Cross-sectional TEM image of the interface between the SiNW and Al_2O_3.

Finally, to estimate the optimal length of a SiNW for effective carrier collection, effective diffusion length of minority carriers was calculated from the obtained minority carrier lifetime. Most of the generated minority carriers have to move to an external circuit by diffusion because the depletion region of silicon solar cells is generally several hundred nanometers [37]. For simplification, SiNW arrays were regarded as a homogeneous film, and the measured carrier lifetime was assumed as

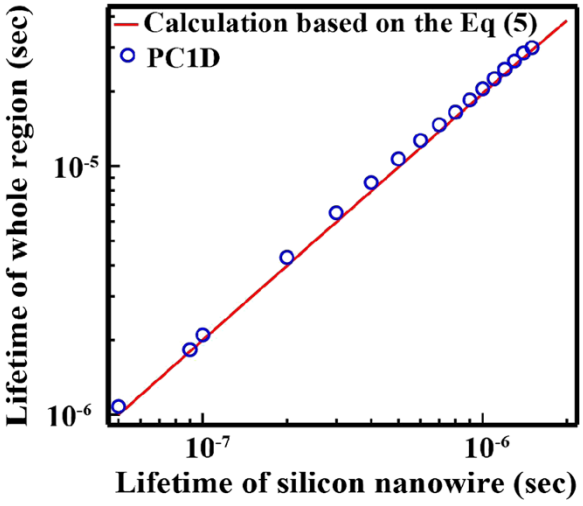

Figure 7 The calculated carrier lifetime. Carrier lifetime in only a SiNW as a function of the carrier lifetime in the whole region by calculation based on Equation 5 and PC1D.

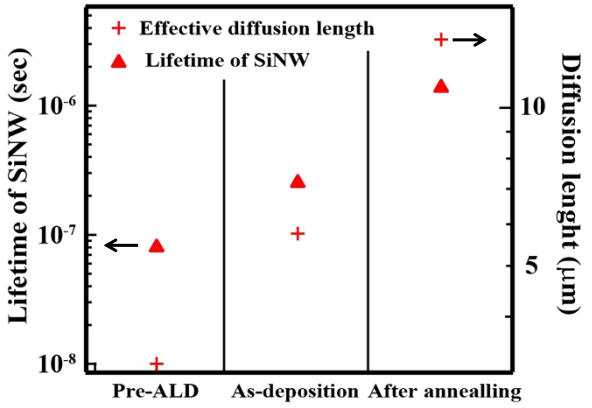

Figure 8 Lifetime and diffusion length in SiNW pre-ALD, as-deposited, and post-annealing.

the bulk lifetime of the homogeneous film. Effective diffusion length (L_e) can be represented by

$$L_e = \sqrt{D\tau} \tag{6}$$

where D is the diffusion coefficient and τ is the bulk lifetime. From the Einstein relation, D is given by

$$D = \frac{kT}{q}\mu \tag{7}$$

where k is the Boltzmann constant, T is the absolute temperature, and q is the elementary charge. μ is the electron mobility of SiNW. The mobility of a SiNW depends on the length, diameter, and fabrication method. Therefore, we use an electron mobility of 51 $cm^2/(V\ s)$ because the SiNW array was fabricated by metal-assisted chemical etching in [25]. When Equation 6 is substituted in Equation 7, this yields the following expression for L_e:

$$L_e = \sqrt{\frac{kT}{q}\mu\tau} \tag{8}$$

Each value was substituted in Equation 8, and effective diffusion length was estimated at 3.25 μm without any passivation films (Figure 8), suggesting that minority carriers around the bottom of the SiNW arrays rapidly recombine, and that is why a very low carrier lifetime of 1.6 μs was obtained. In the case of Al_2O_3 deposited onto SiNW arrays, the diffusion length was estimated to be 5.76 μm, suggesting that passivation effect was not enough to collect minority carriers since there are defects still remaining. After annealing, the effective diffusion length improved to about 13.5 μm. In a heterojunction structure, a depletion region was formed between p-type amorphous Si layer and n-type SiNW. Photogenerated carriers in a SiNW diffuse into the electric region as diffusion current, reach the depletion region, and are collected as photocurrent. If the effective diffusion length is longer than the SiNW length, photogenerated carriers at the bottom region can be also collected as photocurrent. Since 13.5 μm is longer than the length, it is expected that most of the photogenerated carriers can be collected. Therefore, Al_2O_3 deposited by ALD is a promising passivation material for a structure with high aspect ratio such as p-type SiNW arrays. Moreover, it is effective to use a fixed charge in the passivation of SiNW arrays with dangling bonds.

Conclusions

We successfully prepared SiNW arrays embedded in Al_2O_3 by using the MACES technique and the subsequent ALD deposition. HAADF-STEM clearly indicates that the SiNW was completely covered with Al_2O_3. This ALD-Al_2O_3 passivation film reduced surface recombination velocity at the surface of SiNW. The as-deposited Al_2O_3 increased minority carrier lifetime in the sample from 1.6 to 5 μs. Moreover, the lifetime improved up to 27 μs after annealing. These results indicate that ALD-Al_2O_3 is beneficial for the passivation of SiNW surfaces. In addition, we analyzed lifetime data in details to estimate minority carrier diffusion length of the SiNW region. According to the data analysis, we finally derived a simple analytical equation to extract the lifetime of the SiNW region from measured effective lifetime of the samples. Using the equation, it was found that the effective diffusion length of minority carriers in the SiNW array increased from 3.25 to 13.5 μm by depositing Al_2O_3 and post-annealing at 400°C. This improvement of the diffusion length is very important for application to solar cells. The larger diffusion length leads to better carrier collection in solar cells, and improvement of short-circuit current can be expected.

Competing interests

The authors declare that they have no competing interests.

Authors' contributions

SK, YK, YW, and SM carried out the experiment and calculations. AY supervised the work and finalized the manuscript. YO, YN, and MH gave the final approval of the version of the manuscript to be published. All authors read and approved the final manuscript.

Acknowledgements

This work was supported in part by JST, PRESTO, and the Nissan Foundation for Promotion of Science.

Author details

[1]Department of Physical Electronics, Tokyo Institute of Technology, Meguro-ku, Tokyo 152-8552, Japan. [2]PRESTO, Japan Science and Technology Agency (JST), Tokyo 102-0076, Japan. [3]Photovoltaics Research Center (PVREC), Tokyo Institute of Technology, Tokyo 152-8550, Japan. [4]Advanced Materials Laboratory, Nissan Research Center, Yokosuka, Kanagawa 237-8523, Japan.

Received: 7 May 2013 Accepted: 5 August 2013
Published: 23 August 2013

References

1. Kurokawa Y, Kato S, Watanabe Y, Yamada A, Konagai M, Ohta Y, Niwa Y, Hirota M: **Numerical approach to the investigation of performance of silicon nanowire solar cells embedded in a SiO_2matrix.** *Jpn J Appl Phys* 2012, **51:**11PE12.
2. Tsakalakos L, Balch J, Fronheiser J, Shih MY, LeBoeuf SF, Pietrzykowski M, Codella PJ, Korevaar BA, Sulima O, Rand J, Davuluru A, Rapol UD: **Strong broadband optical absorption in silicon nanowire films.** *J Nanophotonics* 2007. doi:10.1117/1.2768999.
3. Lin CX, Povinelli ML: **Optical absorption enhancement in silicon nanowire arrays with a large lattice constant for photovoltaic applications.** *Opt Express* 2009, **17:**19371–19381.
4. Zhu J, Yu ZF, Burkhard GF, Hsu CM, Connor ST, Xu YQ, Wang Q, McGehee M, Fan SH, Cui Y: **Optical absorption enhancement in amorphous silicon nanowire and nanocone arrays.** *Nano Lett* 2009, **9:**279–282.
5. William S, Hans JQ: **Detailed balance limit of the efficiency of p-n junction solar cells.** *J Appl Phys* 1961, **32:**510–519.
6. Kato S, Kurokawa Y, Watanabe Y, Yamada Y, Yamada A, Ohta Y, Niwa Y, Hirota M: **Optical assessment of silicon nanowire arrays fabricated by metal-assisted chemical etching.** *Nanoscale Res Lett* 2013, **8:**216.
7. Hochbaum AI, Fan R, He RR, Yang PD: **Controlled growth of Si nanowire arrays for device integration.** *Nano Lett* 2005, **5:**457–460.
8. Wang N, Tang YH, Zhang YF, Lee CS, Bello I, Lee ST: **Si nanowires grown from silicon oxide.** *Chem Phys Lett* 1999, **299:**237–242.
9. Westwater J, Gosain DP, Tomiya S, Usui S, Ruda H: **Growth of silicon nanowires via gold/silane vapor–liquid–solid reaction.** *J Vac Sci Technol B* 1997, **15:**554–557.
10. Peng KQ, Zhang ML, Lu AJ, Wong NB, Zhang RQ, Lee ST: **Ordered silicon nanowire arrays via nanosphere lithography and metal-induced etching.** *Appl Phys Lett* 2007, **90:**163123.
11. Zhang ML, Peng KQ, Fan X, Jie JS, Zhang RQ, Lee ST, Wong NB: **Preparation of large-area uniform silicon nanowires arrays through metal-assisted chemical etching.** *J Phys Chem C* 2008, **112:**4444–4450.
12. Liu HI, Maluf NI, Pease RFW, Biegelsen DK, Johnson NM, Ponce FA: **Oxidation of sub-50 nm Si columns for light-emission study.** *J Vac Sci Technol B* 1992, **10:**2846–2850.
13. Ono T, Saitoh H, Esashi M: **Si nanowire growth with ultrahigh vacuum scanning tunneling microscopy.** *Appl Phys Lett* 1997, **70:**1852–1854.
14. Chen C, Jia R, Yue HH, Li HF, Liu XY, Wu DQ, Ding WC, Ye TC, Kasai S, Tamotsu H, Chao J, Wang S: **Silicon nanowire-array-textured solar cells for photovoltaic application.** *J Appl Phys* 2010, **108:**094318.
15. Shiu SC, Chao JJ, Hung SC, Yeh CL, Lin CF: **Morphology dependence of silicon nanowire/poly(3,4-ethylenedioxythiophene):poly(styrenesulfonate) heterojunction solar cells.** *Chem Mater* 2010, **22:**3108–3113.
16. Sivakov V, Andra G, Gawlik A, Berger A, Plentz J, Falk F, Christiansen SH: **Silicon nanowire-based solar cells on glass: synthesis, optical properties, and cell parameters.** *Nano Lett* 2009, **9:**1549–1554.
17. Lu YR, Lal A: **High-efficiency ordered silicon nano-conical-frustum array solar cells by self-powered parallel electron lithography.** *Nano Lett* 2010, **10:**4651–4656.
18. Garnett EC, Yang PD: **Silicon nanowire radial p-n junction solar cells.** *J Am Chem Soc* 2008, **130:**9224–9225.
19. Kempa TJ, Tian BZ, Kim DR, Hu JS, Zheng XL, Lieber CM: **Single and tandem axial p-i-n nanowire photovoltaic devices.** *Nano Lett* 2008, **8:**3456–3460.
20. Dan Y, Seo K, Takei K, Meza JH, Javey A, Crozier KB: **Dramatic reduction of surface recombination by in situ surface passivation of silicon nanowires.** *Nano Letters* 2011, **11:**2527–2532.
21. Demichel O, Calvo V, Besson A, Noé P, Salem B, Pauc N, Oehler F, Gentile P, Magnea N: **Surface recombination velocity measurements of efficiently passivated gold-catalyzed silicon nanowires by a new optical method.** *Nano Letters* 2010, **10:**2323–2329.
22. Peng KQ, Huang ZP, Zhu J: **Fabrication of large-area silicon nanowire p–n junction diode arrays.** *Adv Mater* 2004, **16:**73–76.
23. Kato S, Watanabe Y, Kurokawa Y, Yamada A, Ohta Y, Niwa Y, Hirota M: **Metal-assisted chemical etching using silica nanoparticle for the fabrication of a silicon nanowire array.** *Jpn J Appl Phys* 2012, **51:**02BP09–02BP09-4.
24. Fang H, Li X, Song S, Xu Y, Zhu J: **Fabrication of slantingly-aligned silicon nanowire arrays for solar cell applications.** *Nanotechnology* 2008, **19:**255703.
25. Hui F, Li X, Song S, Xu Y, Zhu J: **Fabrication of slantingly-aligned silicon nanowire arrays for solar cell applications.** *Nanotechnology* 2008, **19:**255703.
26. Schmidt J, Merkle A, Brendel R, Hoex B, van de Sanden MCM, Kessels WMM: **Surface passivation of high-efficiency silicon solar cells by atomic-layer-deposited Al_2O_3.** *Prog Photovoltaics* 2008, **16:**461–466.
27. Agostinelli G, Delabie A, Vitanov P, Alexieva Z, Dekkers HFW, De Wolf S, Beaucarne G: **Very low surface recombination velocities on p-type silicon wafers passivated with a dielectric with fixed negative charge.** *Sol Energ Mat Sol C* 2006, **90:**3438–3443.
28. Poodt P, Lankhorst A, Roozeboom F, Spee K, Maas D, Vermeer A: **High-speed spatial atomic-layer deposition of aluminum oxide layers for solar cell passivation.** *Adv Mater* 2010, **22:**3564.
29. Saint-Cast P, Benick J, Kania D, Weiss L, Hofmann M, Rentsch J, Preu R, Glunz SW: **High-efficiency c-Si solar cells passivated with ALD and PECVD aluminum oxide.** *IEEE Electr Device L* 2010, **31:**695–697.
30. Saint-Cast P, Kania D, Hofmann M, Benick J, Rentsch J, Preu R: **Very low surface recombination velocity on p-type c-Si by high-rate plasma-deposited aluminum oxide.** *Appl Phys Lett* 2009, **95:**151502.
31. Bowden S, Sinton RA: **Determining lifetime in silicon blocks and wafers with accurate expressions for carrier density.** *J Appl Phys* 2007, **102**.
32. Bothe K, Krain R, Falster R, Sinton R: **Determination of the bulk lifetime of bare multicrystalline silicon wafers.** *Prog Photovoltaics* 2010, **18:**204–208.
33. Brody J, Rohatgi A, Yelundur V: **Bulk resistivity optimization for low-bulk-lifetime silicon solar cells.** *Prog Photovoltaics* 2001, **9:**273–285.
34. Matsuda A, Nomoto K, Takeuchi Y, Suzuki A, Yuuki A, Perrin J: **Temperature-dependence of the sticking and loss probabilities of silyl radicals on hydrogenated amorphous-silicon.** *Surface Science* 1990, **227:**50–56.
35. Matsuda A, Tanaka K: **Investigation of the growth-kinetics of glow-discharge hydrogenated amorphous-silicon using a radical separation technique.** *J Appl Phys* 1986, **60:**2351–2356.
36. Dingemans G, van de Sanden MCM, Kessels WMM: **Influence of the deposition temperature on the c-Si surface passivation by Al_2O_3films synthesized by ALD and PECVD.** *Electrochem Solid St* 2010, **13:**H76–H79.
37. Mishima T, Taguchi M, Sakata H, Maruyama E: **Development status of high-efficiency HIT solar cells.** *Sol Energ Mat Sol C* 2011, **95:**18–21.

doi:10.1186/1556-276X-8-361
Cite this article as: Kato *et al.*: Improvement of carrier diffusion length in silicon nanowire arrays using atomic layer deposition. *Nanoscale Research Letters* 2013 **8**:361.